

# Simple ultrasonic construction of AgBr/Ag<sub>3</sub>PO<sub>4</sub> hybrid quasi-microcube with improved visible-driven photocatalytic property

Jinsong Xie<sup>1,2</sup>, Difang Zhao<sup>1,2</sup>, Changan Tian<sup>1,2</sup>, Chengliang Han<sup>1,2</sup>, Hui Zhang<sup>1</sup>

<sup>1</sup>Department of Chemistry and Materials Engineering, Hefei University, Hefei 230601, People's Republic of China

<sup>2</sup>Key Laboratory of Powder and Energy Sources Materials, Hefei University, Hefei 230601, People's Republic of China  
E-mail: xjs153@hfu.edu.cn

Published in *Micro & Nano Letters*; Received on 13th March 2013; Accepted on 21st May 2013

AgBr/Ag<sub>3</sub>PO<sub>4</sub> composite quasi-microcubes were fabricated by a simple ultrasonic synthesis method, in which hexadecyltrimethylammonium bromide was used as Br resource and surfactant. The structures and morphologies of the as-obtained product were initially characterised by X-ray diffraction, field emission scanning electron microscopy and energy dispersive X-ray analysis spectroscopy. The ultraviolet–visible diffuse reflectance spectrum of the as-obtained products demonstrated that this hybrid structure exhibits an enhanced absorption ability in the visible region. Furthermore, the composite products exhibit much higher photocatalytic performance and stability on degradation of rhodamine B dye under the stimulated sunlight irradiation compared with pure AgBr and Ag<sub>3</sub>PO<sub>4</sub>.

**1. Introduction:** Nowadays, how to deal with the current environmental and energy problems has attracted much attention by many scientists and they are devoted to exploring novel and effective photocatalysts to address these issues. Among them, as a kind of new type of semiconductor materials, Ag<sub>3</sub>PO<sub>4</sub> nanomaterials with various morphologies have been achieved via different strategies [1–3]. More specifically, Ye research groups demonstrated that Ag<sub>3</sub>PO<sub>4</sub> has excellent abilities to split water and decompose organic dyes through a series of experiments [4]. Furthermore, they found Ag<sub>3</sub>PO<sub>4</sub> with rhombic dodecahedrons structures show much higher activities than cube shapes for the degradation of organic dyes methyl orange and rhodamine B (RhB) [5]. Additionally, hierarchical Ag<sub>3</sub>PO<sub>4</sub> porous microcubes [6], rejuvenate Ag<sub>3</sub>PO<sub>4</sub> [7] and colloidal Ag<sub>3</sub>PO<sub>4</sub> nanocrystals [8, 9] have, respectively, formed, which show excellent visible light activity for the photodecomposition of organic dyes. In order to improve Ag<sub>3</sub>PO<sub>4</sub> visible-driven photocatalytic ability and its stability, there are increasing efforts on combining Ag<sub>3</sub>PO<sub>4</sub> with other materials to form heterostructures, such as semiconductor TiO<sub>2</sub> [10–12], noble metal Ag [13, 14], AgX (X = Cl, Br, I) [15], Fe<sub>3</sub>O<sub>4</sub> [16], carbon quantum dots [17], hydroxyapatite [18] and so on. Up to now, there are few reports on the synthesis of AgBr/Ag<sub>3</sub>PO<sub>4</sub> composite nanostructures by means of a kind of ultrasonic reaction way. In this Letter, for the first time we demonstrate a simple and one-pot ultrasonic method to prepare a AgBr/Ag<sub>3</sub>PO<sub>4</sub> composite nanostructure. This processing method is low cost and easy to manipulate. Furthermore, AgBr nanoparticles can easily adhere to the surface of the Ag<sub>3</sub>PO<sub>4</sub> quasi-cube and form a AgBr/Ag<sub>3</sub>PO<sub>4</sub> composite nanostructure by this way. Furthermore, we can utilise this way to construct other similar inorganic/inorganic heterostructures in future work. The as-obtained products act as excellent candidates for possible application in the waste water disposal field.

## 2. Experimental

**2.1. Preparation of photocatalyst:** All of the reagents are analytic grade with no further purification in our experiment procedure. In a typical process, firstly 0.3 g of NaH<sub>2</sub>PO<sub>4</sub>•2H<sub>2</sub>O was dissolved into 10 ml of H<sub>2</sub>O and stirred for 5 min to form a transparent solution (solution 1). Additionally, 0.2 g of CTAB and 0.51 g of AgNO<sub>3</sub> were added into 10 ml of H<sub>2</sub>O and stirred for 10 min to make them disperse (solution 2). Finally, solution 1 was transferred to solution 2 for ultrasonic reaction for 1 h. Thereafter, the resultant yellow colloids were thoroughly centrifuged and

washed with water and absolute ethanol three times, respectively, and dried in a vacuum oven at 30°C. Pure Ag<sub>3</sub>PO<sub>4</sub> and AgBr were produced in the above conditions by just varying the starting materials. The synthesis parameters of the other products are described in Table 1.

**2.2. Characterisation means:** Powder X-ray diffraction (XRD) measurements were performed on a Bruker D8-advance X-ray diffractometer with Cu K $\alpha$  radiation ( $\lambda = 0.154056$  nm). The field emission scanning electron microscopy (FE-SEM) image and energy dispersive X-ray analysis (EDX) spectra were recorded on a Hitachi S-4800 FE-SEM using an operating voltage of 10 kV. The ultraviolet–visible diffuse reflectance spectrum (UV-DRS) spectra were obtained by a UV-3900 (Hitachi) spectrometer.

**2.3. Photocatalytic tests:** The photocatalytic activity of the products was evaluated by degradation of the RhB solution under a 350 W Xe lamp irradiation. About 50 mg photocatalyst was put into a quartz tube containing 50 ml of  $2 \times 10^{-5}$  M RhB solution. Then, the mixture solution was sonicated for 15 min and stirred in the dark for 60 min to ensure adsorption/desorption equilibrium between the catalyst and dye. After that, the mixture solution was constantly stirring under 350 W Xe lamps. About 3 ml of the suspension was collected and centrifuged to discard the catalyst after the given time of 5 min. Finally, the concentration of the RhB solution was measured by a Shimadzu 2550 UV–visible spectrophotometer.

**3. Results and discussion:** The crystalline phase and chemical composition of S1 are determined by the XRD pattern as indicated in Fig. 1. It is easily observed that all the diffraction peaks belong to two kinds of compounds. The peaks labelled with ‘▼’ can be easily indexed to cubic phase Ag<sub>3</sub>PO<sub>4</sub>, which are well matched to the standard data (JCPDF Card No. 060505).

**Table 1** Synthesis parameters of the products S1, S2 and S3

Sample number	Products	Reaction time, h	Sonication power, W
S1	AgBr/Ag <sub>3</sub> PO <sub>4</sub>	0.5	300
S2	AgBr/Ag <sub>3</sub> PO <sub>4</sub>	1	300
S3	AgBr/Ag <sub>3</sub> PO <sub>4</sub>	1.5	300

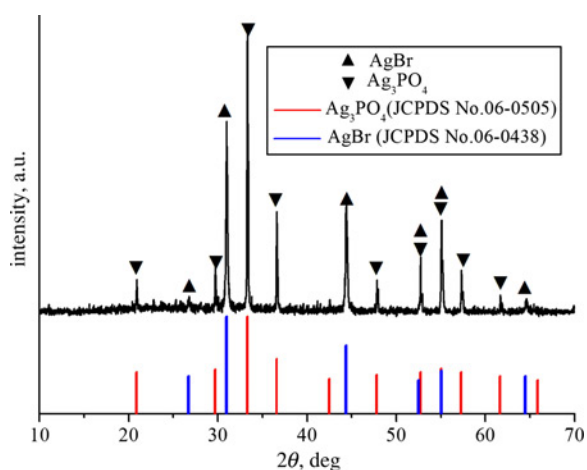


**Figure 1** XRD pattern of S2

The other peaks marked ‘▲’ confirm cubic phase AgBr in light of the standard data (JCPDF Card No. 060438). No other reflections are observed in Fig. 1, indicating the obtained products were completely consisted of Ag<sub>3</sub>PO<sub>4</sub> and AgBr.

The FE-SEM images of S2 are illustrated in Figs. 2a and b. The as-obtained S1 exhibited a representative microcube structure with a rough surface. From a magnified FE-SEM image, we can easily find that the products indeed are composed of quasi-cubes with the diameter of about 1 μm and sphere-like nanoparticles with the size about 0.1 μm embedded on their surfaces. In order to specify the chemical composition of the hybrid quasi-cubic S1, we characterised it by the EDX spectrum as shown in Fig. 2b. The peaks of Ag, P, Br, O and C elements can be detected. The peaks of trace Au may come from substrate for SEM detection. Additionally, the FE-SEM images of pure Ag<sub>3</sub>PO<sub>4</sub> and AgBr are also, respectively, given as Figs. 3c and d. Obviously, the as-formed Ag<sub>3</sub>PO<sub>4</sub> has a cubic appearance and AgBr has a dispersive nanosphere configuration. Associated with the XRD pattern, we can further confirm that the as-obtained heterostructure products consist of cubic

Ag<sub>3</sub>PO<sub>4</sub> and AgBr nanoparticles. Furthermore, the FE-SEM images of the products under the reaction time of 0.5 or 1.5 h are also given in Figs. 3a and b. There are lots of AgBr nanoparticles irregularly dispersed on the surface of the bulk Ag<sub>3</sub>PO<sub>4</sub> materials. With prolonging the reaction time to 1.5 h, the morphology of the obtained Ag<sub>3</sub>PO<sub>4</sub> transferred from cubes into triangles. The sizes of Ag<sub>3</sub>PO<sub>4</sub> are obviously increased to nearly 5 μm as shown in Fig. 3b. From the above experiment results, the preferable reaction time is 1 h.

The UV-DRS of the AgBr/Ag<sub>3</sub>PO<sub>4</sub> heterostructure quasi-cube (S2) is presented in Fig. 4. It can be easily found that the obtained AgBr/Ag<sub>3</sub>PO<sub>4</sub> heterostructure quasi-cube exhibits excellent optical absorbance during 250–550 nm. Furthermore, the absorption edge of the heterostructure quasi-cube has been extended to around 545 nm, which is larger than the reported absorption edge ca. 520 nm of the pure Ag<sub>3</sub>PO<sub>4</sub> cube [5]. These above results demonstrated that the obtained heteroproducts might have stronger visible harvesting capacity and better visible-driven photodegradation of organic dyes compared with the single cubic Ag<sub>3</sub>PO<sub>4</sub>.

The photocatalytic performances of the various samples under the same simulated sunlight irradiation conditions are presented as shown in Fig. 5. In general, under the same irradiation time, the degradation efficiency of RhB dye is differing because of the change of the catalyst. Without the catalyst, the self-degradation of RhB dye is nearly ignored under the simulated sunlight irradiation as displayed in Fig. 5. When using the AgBr/Ag<sub>3</sub>PO<sub>4</sub> heterostructure quasi-cube (S2) as photocatalyst, the RhB dye is drastically decomposed and photodegradation efficiency reached 98% under the simulated sunlight irradiation for 20 min, which displayed enhanced photocatalytic efficiency compared with pure Ag<sub>3</sub>PO<sub>4</sub> or AgBr as photocatalyst under the same catalytic conditions. Additionally, the photocatalytic abilities of the samples S1 and S3 were also investigated. The results show the degradation efficiency of the samples S1 and S3 is, respectively, about 70 and 63% as illustrated in Fig. 5 in the same conditions, which are lower than the photodegradation efficiency of S2. The catalytic efficiency difference among the S1, S3 and S3 may be attributed to the gathering degree and size of AgBr and Ag<sub>3</sub>PO<sub>4</sub> as shown in Figs. 3a and b.

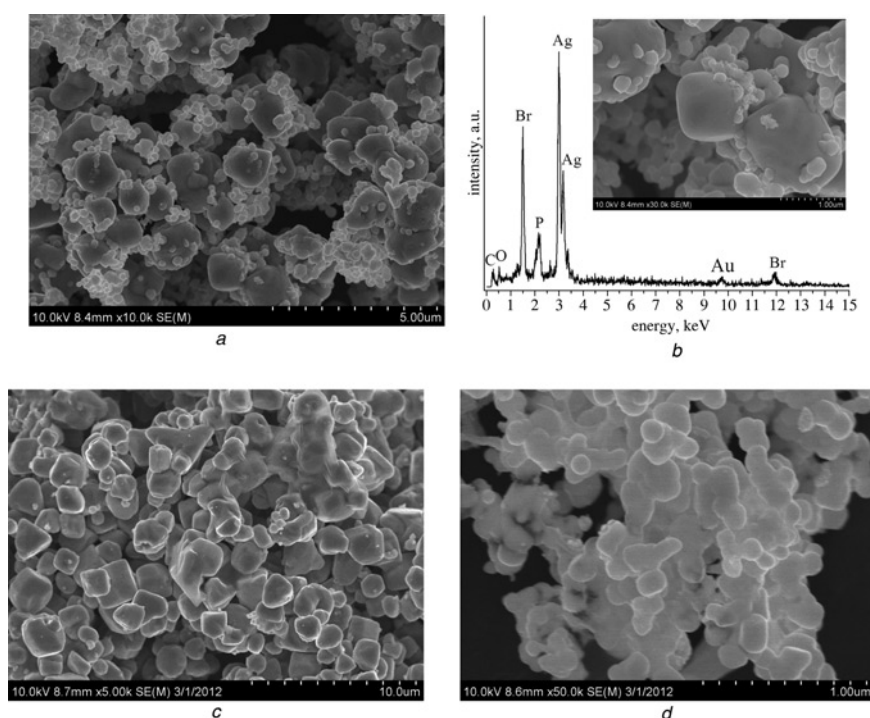


**Figure 2** FE-SEM images (Figs. 2a and b) and EDX spectrum (Fig. 2b) of S2; FE-SEM images of pure Ag<sub>3</sub>PO<sub>4</sub> (Fig. 2c) and AgBr (Fig. 2b)

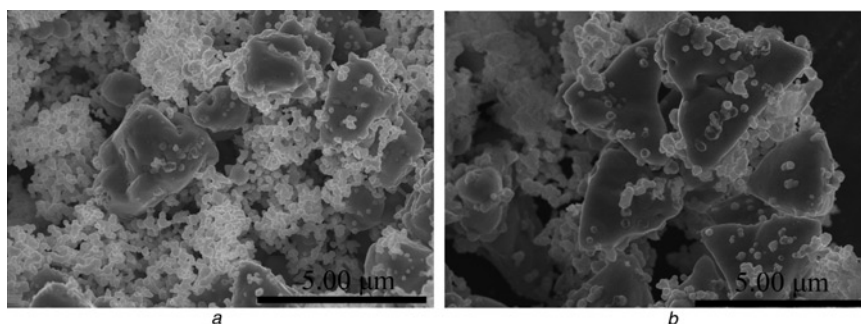


Figure 3 FE-SEM image of S1 (Fig. 3a) and S3 (Fig. 3b)

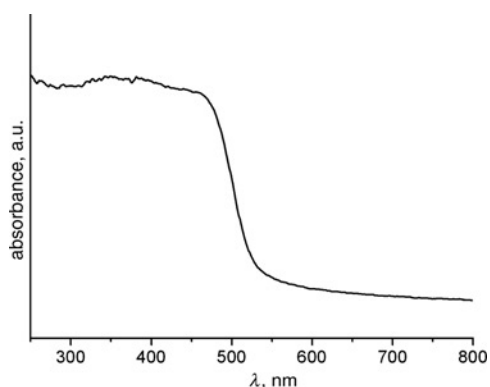


Figure 4 UV-visible diffusive reflectance spectrum of S2

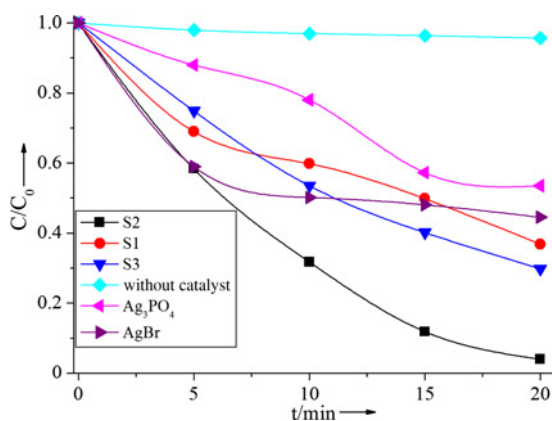


Figure 5 Photocatalytic performances of S1, S2, S3, Ag<sub>3</sub>PO<sub>4</sub>, AgBr and without catalyst for photodecomposition of RhB solution under the simulated sunlight irradiation

**4. Conclusions:** In summary, a kind of AgBr/Ag<sub>3</sub>PO<sub>4</sub> hybrid quasi-cube is prepared via a polymer-associated-ultrasonic and “green” method. Moreover, the obtained AgBr/Ag<sub>3</sub>PO<sub>4</sub> hybrid quasi-cube showed better photocatalytic degradation of RhB solution under the stimulated sunlight irradiation compared with the single AgBr or Ag<sub>3</sub>PO<sub>4</sub>, and has a possible application in the treatment of polluted water. More importantly, this synthesis strategy can further construct other Ag<sub>3</sub>PO<sub>4</sub>-based binary and ternary hybrids with enhanced visible-driven photocatalytic ability.

**5. Acknowledgments:** The authors acknowledge financial support from the National Natural Science Foundation of China (grant no.

51102073), the Natural Science Foundation of Anhui Province (grant numbers 1308085QB35, 10040606Q53, 11040606M100 and 1308085QB30), the Natural Science Foundation of the Education Department of Anhui Province (grant numbers KJ2012B154 and KJ2012B148) and the Natural Science Foundation of Hefei University (grant no. 12RC02).

## 6 References

- [1] Thomas M., Ghosh S.K., George K.C.: ‘Characterisation of nano-structured silver orthophosphate’, *Mater. Lett.*, 2002, **56**, pp. 386–392
- [2] Bi Y.P., Hu H.Y., Ouyang S.X., Lu G.X., Cao J.Y., Ye J.H.: ‘Photocatalytic and photoelectric properties of cubic Ag<sub>3</sub>PO<sub>4</sub> sub-microcrystals with sharp corners and edges’, *Chem. Commun.*, 2012, **48**, pp. 3748–3750
- [3] Wang W.G., Cheng B., Yu J.G., Liu G., Fan W.H.: ‘Visible-light photocatalytic activity and deactivation mechanism of Ag<sub>3</sub>PO<sub>4</sub> spherical particle’, *Chem. Asian J.*, 2012, **7**, pp. 1902–1908
- [4] Yi Z.G., Ye J.H., Naoki K., *ET AL.*: ‘An orthophosphate semiconductor with photooxidation properties under visible-light irradiation’, *Nat. Mater.*, 2010, **9**, pp. 559–564
- [5] Bi Y.P., Ouyang S.X., Umezawa N., Cao J.Y., Ye J.H.: ‘Facet effect of single-crystalline Ag<sub>3</sub>PO<sub>4</sub> sub-microcrystals on photocatalytic properties’, *J. Am. Chem. Soc.*, 2011, **133**, pp. 6490–6492
- [6] Liang Q.H., Ma W.J., Shi Y., Li Z., Yang X.M.: ‘Hierarchical Ag<sub>3</sub>PO<sub>4</sub> porous microcubes with enhanced photocatalytic properties synthesized with the assistance of trisodium citrate’, *CrystEngComm*, 2012, **14**, pp. 2966–2973
- [7] Wang H., Bai Y.S., Yang J.T., Lang X.F., Li J.H., Guo L.: ‘A facile way to rejuvenate Ag<sub>3</sub>PO<sub>4</sub> as a recyclable highly efficient photocatalyst’, *Chem. Eur. J.*, 2012, **18**, pp. 5524–5529
- [8] Dinh C.T., Nguyen T.D., Kleitz F., Do T.O.: ‘Large-scale synthesis of uniform silver orthophosphate colloidal nanocrystals exhibiting high visible light photocatalytic activity’, *Chem. Commun.*, 2011, **47**, pp. 7797–7799
- [9] Khan A., Qamar M., Muneer M.: ‘Synthesis of highly active visible-light-driven colloidal silver orthophosphate’, *Chem. Phys. Lett.*, 2012, **54–58**, pp. 519–520
- [10] Yao W.F., Zhang B., Huang C.P., Ma C., Song X.L., Xu Q.J.: ‘Synthesis and characterization of high efficiency and stable Ag<sub>3</sub>PO<sub>4</sub>/TiO<sub>2</sub> visible light photocatalyst for the degradation of methylene blue and rhodamine B solutions’, *J. Mater. Chem.*, 2012, **22**, pp. 4050–4055
- [11] Rawal S.B., Sung S.D., Lee W.I.: ‘Novel Ag<sub>3</sub>PO<sub>4</sub>/TiO<sub>2</sub> composites for efficient decomposition of gaseous 2-propanol under visible-light irradiation’, *Catal. Commun.*, 2012, **17**, pp. 131–135
- [12] Liu R.Y., Hu P.G., Chen S.W.: ‘Photocatalytic activity of Ag<sub>3</sub>PO<sub>4</sub> nanoparticle/TiO<sub>2</sub> nanobelt heterostructures’, *Appl. Surf. Sci.*, 2012, **258**, pp. 9805–9809
- [13] Liu Y.P., Fang L., Lu H.D., Liu L.J., Wang H., Hu C.Z.: ‘Highly efficient and stable Ag/Ag<sub>3</sub>PO<sub>4</sub> plasmonic photocatalyst in visible light’, *Catal. Commun.*, 2012, **17**, pp. 200–204
- [14] Bi Y.P., Hu H.Y., Ouyang S.X., Jiao Z.B., Lu G.X., Ye J.H.: ‘Selective growth of Ag<sub>3</sub>PO<sub>4</sub> submicro-cubes on Ag nanowires to fabricate necklace-like heterostructures for photocatalytic applications’, *J. Mater. Chem.*, 2012, **22**, pp. 14847–14850
- [15] Bi Y.P., Ouyang S.X., Cao J.Y., Ye J.H.: ‘Facile synthesis of rhombic dodecahedral AgX/Ag<sub>3</sub>PO<sub>4</sub> (X = Cl, Br, I) heterocrystals with

- enhanced photocatalytic properties and stabilities', *Phys. Chem. Chem. Phys.*, 2011, **13**, pp. 10071–10075
- [16] Li G.P., Mao L.Q.: 'Magnetically separable  $\text{Fe}_3\text{O}_4$ - $\text{Ag}_3\text{PO}_4$  sub-micrometre composite: facile synthesis, high visible light-driven photocatalytic efficiency, and good recyclability', *R. Soc. Chem. Adv.*, 2012, **2**, pp. 5108–5111
- [17] Zhang H.C., Huang H., Ming H., *ET AL.*: 'Carbon quantum dots/ $\text{Ag}_3\text{PO}_4$  complex photocatalysts with enhanced photocatalytic activity and stability under visible light', *J. Mater. Chem.*, 2012, **22**, pp. 10501–10506
- [18] Hong X.T., Wu X.H., Zhang Q.Y., *ET AL.*: 'Hydroxyapatite supported  $\text{Ag}_3\text{PO}_4$  nanoparticles with higher visible light photocatalytic activity', *Appl. Surf. Sci.*, 2012, **258**, pp. 4801–4805